A Broadband Polynomial Predistorter for Reconfigurable Radio

T. Nesimoglu, C. N. Canagarajah and J. P. McGeehan

University of Bristol
Department of Electrical and Electronic Engineering, Room 2.14,
Queens Building, University Walk, Bristol, BS8 1TR, UK
Tel: +(44) 117 928 8618 Fax: +(44) 117 954 5206
Email: T.Nesimoglu@Bristol.ac.uk

Abstract

An analogue polynomial predistorter working at RF is presented. It is capable of operating at multiple frequency bands over a wide linearisation bandwidth. These are important features for a reconfigurable radio application. The technique approximates the inverse of the amplifiers transfer function up to third-order (cubic) nonlinearity by using polynomial functions. Theoretical analysis shows that the performance of the technique is limited more by the generation of additional fifth-order IMD (IM5), than the gain and phase matching of the predistorter. The measured two-tone tests at different frequency bands show 13 dB suppression of third-order IMD (IM3) is possible over 40 MHz tone separation. A 30 dB IM3 reduction can be achieved by increasing the IM5 by 9 dB. The research will continue by extending the predistorter to include higher orders of nonlinearity for a larger improvement in IMD suppression.

I. Introduction

The efficient utilization of allocated spectrum for mobile and wireless communication systems is an important issue. Both 2G spectrum efficient modulation schemes such as $\pi/4$-DQPSK and 3G W-CDMA have envelope variations. If these signals are applied to a power amplifier (PA), the performance of the communication system will be degraded by spreading of the output spectrum into adjacent channels causing interference to the others and violating the emission specifications. In order to reduce this Adjacent Channel Interference (ACI) the guard-band has to be increased, thus reducing the number of channels in the available bandwidth. In a receiver, ACI will make it more difficult or even impossible to isolate the desired signal and correctly detect the transmitted data.

The new 3G systems will also offer the services of 2G. Although 3G services will be active throughout the world, a worldwide unification of multiple standards could not be established. Dual-mode handsets have partially solved the problem until the migration from GSM to UMTS is complete, but multimode operation within the 3G will still be inevitable for global roaming. A smart solution is a reconfigurable receiver, so called software defined radio (SDR). In the receiver a linear low noise amplifier is required to prevent the out of band blocker signal from producing in band interference, and in the transmitter a linear PA prevents spurious emissions. The design of a suitable amplifier linearisation technique is a challenging task for the RF engineer. The candidate linearisation scheme should:

- Operate at RF over multiple frequency bands, and have a wide linearisation bandwidth.
- Be independent of the modulation scheme, so that different standards can be transmitted or received.
- Have high power efficiency and simple circuitry.

Analogue predistortion [1, 2] and feedforward [3] are suitable for both multiband and broadband applications. Feedforward can provide large improvements in linearity but the overall efficiency of the system is low, where analogue predistortion can be more efficient due to smaller circuitry. Analogue predistorters operating at IF [4, 5] have shown good performance. However, a reconfigurable radio front-end would require a broadband predistorter at RF.

II. Theory of Polynomial Predistortion

The block diagram of a cubic predistorter is shown in Fig.1. The input signal is separated into two paths; one passing through the linear and the other through the nonlinear path, where the cubic nonlinearity is introduced. The output of the nonlinear path is the cubicly distorted version of the input signal; thus it contains *IM3* products. The output of the linear path is the amplitude and phase

0-7803-6728-6/01/$10.00 ©2001 IEEE.

adjusted replica of the input signal. The variable attenuator on the linear path is adjusted so that the PA operates near the saturation point. The delay matching of the two loops is important for broadband linearisation; therefore the linear path contains a variable delay line to compensate for the transit-time through various elements in the nonlinear path. The variable attenuator and phase shifter on the nonlinear path are set to assure the correct cubic nonlinearity is achieved for the optimum *IM3* cancellation at the output of the amplifier. The outputs of the two paths are combined and then applied to the input of the PA. The input signal for a general two-tone test with equal amplitudes is given in Equation 1.

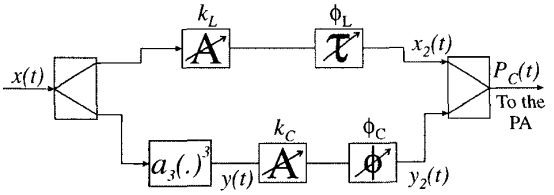

Figure 1. A cubic predistorter block diagram.

$$x(t) = A\left[\cos(\omega_1 t) + \cos(\omega_2 t)\right] \tag{1}$$

This signal is split and applied to the cubic nonlinearity generating element with the transfer function described as in Equation 2. After substituting Equation 1 and expanding, the resulting signal is given in Equation 3, which is simplified by considering only the fundamentals and inband *IM3* products appearing adjacent to these fundamentals. Also, since the frequency separation is small, amplitude and phase adjustment is assumed to be equal through the whole bandwidth of interest.

$$y(t) = a_3[x(t)]^3 \tag{2}$$

$$y_2(t) = \frac{3}{4}a_3 k_C A^3 \left\{ \begin{matrix} 3\left[\cos(\omega_1 t + \phi_C) + \cos(\omega_2 t + \phi_C)\right] + \\ \cos(2\omega_1 t - \omega_2 t + \phi_C) + \cos(2\omega_2 t - \omega_1 t + \phi_C) \end{matrix} \right\} \tag{3}$$

where k_C is the amplitude adjustment controlled by the attenuator and $\varnothing_C$ is the phase shift introduced by the phase shifter on the cubic path. The output signal of the linear path is shown in Equation 4, where k_L is the amplitude adjustment and $\varnothing_L$ is the phase shift introduced by the variable delay line. The outputs of the linear and nonlinear paths will be combined as shown in Equation 5, and applied to the input of the PA.

$$x_2(t) = k_L A\left[\cos(\omega_1 t + \phi_L) + \cos(\omega_2 t + \phi_L)\right] \tag{4}$$

$$\begin{aligned} P_C(t) &= x_2(t) + y_2(t) \\ &= k_L A\left[\cos(\omega_1 t + \phi_L) + \cos(\omega_2 t + \phi_L)\right] + \\ &\quad \frac{3}{4}a_3 k_C A^3 \left\{ \begin{matrix} 3\left[\cos(\omega_1 t + \phi_C) + \cos(\omega_2 t + \phi_C)\right] \\ + \begin{pmatrix} \cos(2\omega_1 t - \omega_2 t + \phi_C) + \\ \cos(2\omega_2 t - \omega_1 t + \phi_C) \end{pmatrix} \end{matrix} \right\} \end{aligned} \tag{5}$$

The cubic predistorter will theoretically alter the third-order nonlinearity of the amplifier. Therefore, third-order nonlinearity is considered as the dominant nonlinearity, thus the amplifiers transfer function can be given as in Equation 6. Considering a higher order amplifier transfer function will enable the analysis to show the effects of cubic predistortion on the higher order IMD products more accurately, but this would make the expansion and derivation of the terms extremely difficult.

$$P_A(t) = d_1 P_C(t) + d_3[P_C(t)]^3 \tag{6}$$

By substitution of Equation 5 and after expansion, a large number of terms are obtained; here only the terms appearing at third and fifth-order IMD frequencies will be shown. The *IM3* components are:

$$\begin{aligned} IM3(t) &= \frac{3}{4}d_1 A^3 a_3 k_C \left[\cos(2\omega_1 t - \omega_2 t + \phi_C) + \cos(2\omega_2 t - \omega_1 t + \phi_C)\right] \\ &\quad + \frac{3d_3}{64} \left\{ \begin{matrix} \left(567A^9 a_3^3 k_C^3 + 120A^5 a_3 k_C k_L^2\right)\begin{bmatrix} \cos(2\omega_1 t - \omega_2 t + \phi_C) + \\ \cos(2\omega_2 t - \omega_1 t - \phi_C) \end{bmatrix} \\ + 60A^5 a_3 k_C k_L^2 \begin{bmatrix} \cos(2\omega_1 t - \omega_2 t - \phi_C + 2\phi_L) + \\ \cos(2\omega_2 t - \omega_1 t + \phi_C - 2\phi_L) \end{bmatrix} + \\ \left(378A^7 a_3^2 k_C^2 k_L + 16A^3 k_L^3\right)\begin{bmatrix} \cos(2\omega_1 t - \omega_2 t + \phi_L) + \\ \cos(2\omega_2 t - \omega_1 t - \phi_L) \end{bmatrix} \\ + 189A^7 a_3^2 k_C^2 k_L \begin{bmatrix} \cos(2\omega_1 t - \omega_2 t + 2\phi_C - \phi_L) + \\ \cos(2\omega_2 t - \omega_1 t - 2\phi_C + \phi_L) \end{bmatrix} \end{matrix} \right\} \end{aligned} \tag{7}$$

and the *IM5* components are:

$$IM5(t) = \frac{9d_3}{64} \left\{ \begin{matrix} \left(81A^9 a_3^3 k_C^3 + 8A^5 a_3 k_C k_L^2\right)\begin{bmatrix} \cos(3\omega_1 t - 2\omega_2 t + \phi_C) + \\ \cos(3\omega_2 t - 2\omega_1 t - \phi_C) \end{bmatrix} \\ + 4A^5 a_3 k_C k_L^2 \begin{bmatrix} \cos(3\omega_1 t - 2\omega_2 t - \phi_C + 2\phi_L) + \\ \cos(3\omega_2 t - 2\omega_1 t + \phi_C - 2\phi_L) \end{bmatrix} + \\ 21A^7 a_3^2 k_C^2 k_L \begin{bmatrix} 2\begin{pmatrix} \cos(3\omega_1 t - 2\omega_2 t + \phi_L) + \\ \cos(3\omega_2 t - 2\omega_1 t - \phi_L) \end{pmatrix} + \\ \begin{pmatrix} \cos(3\omega_1 t - 2\omega_2 t + 2\phi_C - \phi_L) + \\ \cos(3\omega_2 t - 2\omega_1 t - 2\phi_C + \phi_L) \end{pmatrix} \end{bmatrix} \end{matrix} \right\} \tag{8}$$

The *IM3* at the output will be reduced by the vector addition of the same frequency components. This vector addition will take place between the linearly amplified predistorting signals (the terms including d_1) and the *IM3* generated by the cubic nonlinearity of the amplifier (the terms including d_3) when the phases ϕ_C and ϕ_L are optimally adjusted. The *IM3* components at any of the two frequencies ($2\omega_1$-ω_2 or $2\omega_2$-ω_1) are in the form of Equation 9, here only the ones at $2\omega_1$-ω_2 are shown for simplicity.

$$IM3(t) = (B+C)\cos(2\omega_1 t - \omega_2 t + \phi_C) + (D+E+F)\cos(2\omega_1 t - \omega_2 t + \phi_L) + G\cos(2\omega_1 t - \omega_2 t - \phi_C + 2\phi_L) + H\cos(2\omega_1 t - \omega_2 t + 2\phi_C - \phi_L) \quad (9)$$

Where $B,\ldots H$ represent the amplitudes of these signals. The *IM3* with amplitudes (*B, C*) and (*D, E, F*) will have phases controlled only by the phase shifters on the cubic and linear paths respectively, and they represent most of the *IM3* products. It is the vector addition of these components which will dominantly achieve suppression. The other two terms with amplitudes *G* and *H* are generated from the interaction between the fundamental and predistorting signals due to the third-order nonlinearity of the amplifier. While the other signals are optimized, these terms will introduce phase errors and prevent perfect cancellation. Ignoring these terms will enable the analysis to show the maximum possible improvement that can be obtained from an ideal predistorter. This will be achieved when the phases are 180^O offset from each other, and the amplitudes meet the condition: *B+C=D+E+F*. At this point the ratio of the *IM3* to the linearly amplified fundamentals can be calculated by using the Equation 11 (in dBc). The linearly amplified fundamentals are shown as:

$$Fu = d_1 k_C A - d_1 \frac{9}{4} k_C A^3 a_3 \quad (10)$$

$$RMax = 20Log_{10}\left|\frac{(B+C)-(D+E+F)}{Fu}\right|$$

$$= 20Log_{10}\left|\frac{\frac{3}{4}\left(A^3 a_3 d_1 k_C + \frac{567A^9 a_3^3 d_3 k_C^3}{16}\right) - \frac{3d_3}{64}\left(\begin{matrix}378A^7 a_3^2 k_C^2 k_L + 16A^3 k_L^2 \\ +120A^5 a_3 k_C k_L^2\end{matrix}\right)}{d_1 k_C A - d_1 \frac{9}{4} k_C A^3 a_3}\right| \quad (11)$$

A more realistic analysis should consider as many signals as possible. In that case the ratio of the *IM3* to the linearly amplified fundamentals is given by:

$$RIM3 = 20Log_{10}\left|\frac{(B+C+G)-(D+E+F+H)}{Fu}\right|$$

$$= 20Log_{10}\left|\frac{\frac{3}{4}\left(\begin{matrix}A^3 a_3 d_1 k_C + \frac{567A^9 a_3^3 d_3 k_C^3}{16} \\ +\frac{3d_3}{64}\left(60A^5 a_3 k_C k_L^2\right)\end{matrix}\right) - \frac{3d_3}{64}\left(\begin{matrix}378A^7 a_3^2 k_C^2 k_L + 16A^3 k_L^2 + \\ 120A^5 a_3 k_C k_L^2 + 189A^7 a_3^2 k_C^2 k_L\end{matrix}\right)}{d_1 k_C A - d_1 \frac{9}{4} k_C A^3 a_3}\right| \quad (12)$$

An amplifier by its own with a transfer function given as in Equation 6, would produce an *IM3* to fundamental ratio as:

$$RAmp = 20Log_{10}\left|\frac{3A^2 d_3}{4d_1 + 9d_3 A^2}\right| \quad (13)$$

Now the *IM3* to fundamental ratio of these three scenarios; a predistorter without phase errors (*RMax*), a more realistic predistorter considering errors introduced by additional *IM3* (*RIM3*) and an amplifier by its own (*RAmp*) can be calculated, by considering the following parameters:

$$A=0.5,\ a_1=1,\ a_3=-0.1405,\ d_1=1,\ d_3=-0.2093,\ k_L=1$$

The calculated results are shown in Fig. 2. The k_C, which is the gain of the cubic line, is considered to be a variable parameter. The cubic predistorter without phase errors would have a maximum *IM3* performance about –80 dBc with optimum gain adjustment. Compared to the amplifier without predistortion, this is equivalent to an *IM3* suppression of 53 dB. The more realistic predistorter shows a maximum *IM3* performance of about –69 dBc, which is equivalent to an *IM3* suppression of 42 dB. This predistorter requires more power to achieve a lower level of *IM3* suppression. An analysis on the necessary gain and phase matching of an ideal cubic predistorter is presented in [6]. It has been predicted that up to 30 dB of *IM3* reduction can be obtained with 0.5 dB gain and 20^O phase accuracy. This degree of matching is relatively easy to achieve with a manually or automatically controlled system. A feedforward system would require 0.3 dB gain and 2^O of phase accuracy to achieve the same level of IMD suppression [7]. The analysis [6] did not consider *IM5* products. However, our analysis clearly shows that the additional IMD products generated from the interaction of the input signals are also important and they should be considered for a better prediction of the capabilities of the technique.

In this analysis, although both the amplifier and predistorter are considered up to third-order nonlinearity (i.e. an ideal cubic predistorter), undesired *IM5* components shown in Equation 8 were generated by the cubic nonlinearity of the amplifier, and the performance of this technique is limited more by these than the gain and phase matching of the predistorting signals. Previously it was assumed that an *ideal* cubic predistorter would *only* affect the *IM3* of an amplifier, but this analysis proves the opposite. In practice, both the predistorter and amplifier will also introduce fifth-order nonlinearity and the number of these undesired *IM5* would be higher than shown in Equation 8. The similar procedure can be applied to calculate the ratio of the *IM5* to fundamental signals (*RIM5*) as the gain of the predistorter changes. This ratio can be calculated by using Equation 14. The behavior of the *IM5* is shown also in Fig.2. As the gain and phase of the predistorter is adjusted for suppressing *IM3*, the *IM5* will increase. Reducing *IM3* below the level of the *IM5* does not bring any advantage, especially if this has been achieved by increasing the level of the *IM5*. This problem will be practically demonstrated by the prototype build by the author.

$$RIM5 = 20Log_{10}\left|\frac{81A^9a_3^3k_C^3 + 8A^5a_3k_Ck_L^3 - 42A^7a_3^2k_C^2k_L}{d_1k_CA - d_1\frac{9}{4}k_CA^3a_3}\right| \quad (14)$$

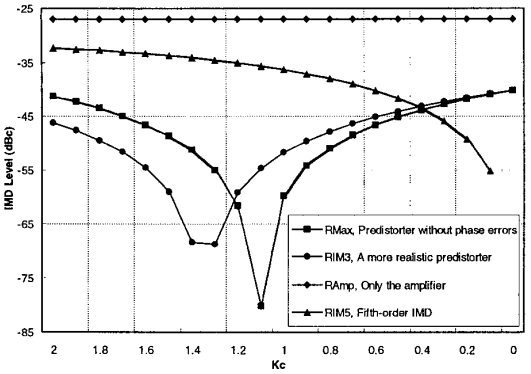

Figure 2. Third and fifth IMD to fundamental ratio with varying gain from the cubic predistorter

III. Practical Predistorter

The cubic nonlinearity generating element is shown in Fig.3. It was constructed by using two cascaded Mini-Circuits double-balanced mixers and two attenuators to drive the mixers within their specified regions. The LO ports were driven at the correct input power to minimize the conversion loss, where the IF ports were well below the LO to prevent saturation. This would help to minimize the level of the undesired IMD products at the output. The amplifier under test can operate up to 1 GHz and produce 1 W output power. The mixers in the circuit have to be capable of operating at twice the highest frequency that the amplifier is aimed for. This is because of the availability of the second-harmonic products $x^2(t)$, in the generation of the *IM3*.

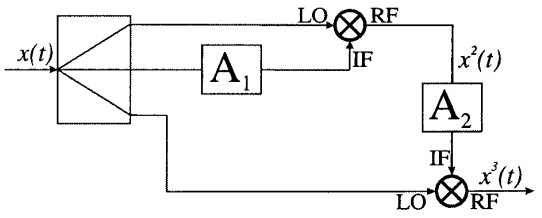

Figure 3. The cubic nonlinearity generator.

Two-tone test with 1 MHz tone separation at 900 MHz yields about 30 dB of *IM3* suppression. However, this has increased the higher order products as shown in Fig. 4. The predistorter can be optimized for a compromise point, where the *IM3* are reduced to the level of these products. This is shown in Fig. 5, where the tone separation is set to 40 MHz at 400 MHz. The *IM3* improvement is about 13 dB. The predistorter has also been tested with π/4–DQPSK and W-CDMA at 450 MHz and 900 MHz respectively. The results are shown in Fig. 6 and Fig. 7. The ACI suppression is modest and similar to the two-tone tests; the *IM3* zone is reduced, while the higher orders are slightly increased.

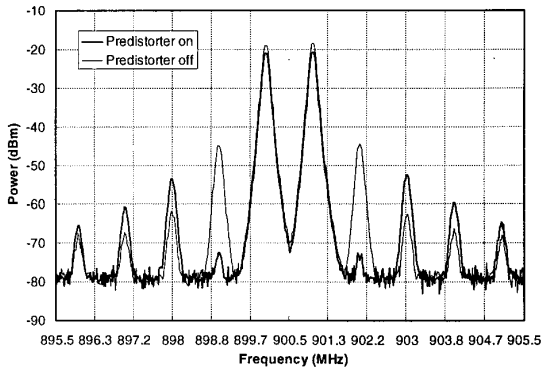

Figure 4. Two-tone test at 900 MHz with 1 MHz tone separation optimized for maximum *IM3* suppression.

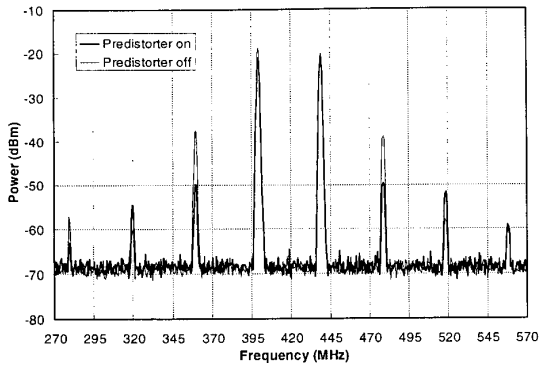

Figure 5. Two-tone test at 400 MHz with 40 MHz tone separation optimized for a compromised *IM3* suppression.

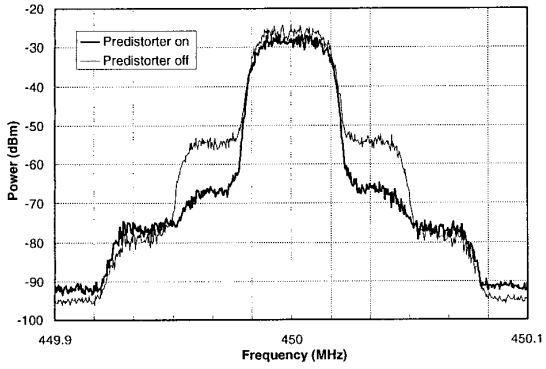

Figure 6. Measured $\pi/4$-DQPSK output spectrum with and without predistorter at 450 MHz.

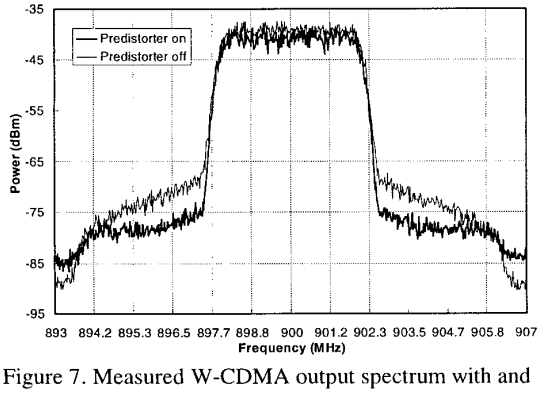

Figure 7. Measured W-CDMA output spectrum with and without predistorter at 900 MHz.

IV. Conclusion

Theoretical analysis has shown that an ideal cubic predistorter would also affect the *IM5* products at the output of an amplifier, and in a practical system this would be the factor limiting the performance. The practical measurements show that up to 30 dB *IM3* reduction is possible by increasing the *IM5* by 9 dB. If the predistorter can be extended to include higher orders of nonlinearity, a large improvement in ACI suppression is expected. The prototype has been tested over different frequency bands up to 40 MHz tone separation. The linearisation bandwidth and multi-band operation is impressive and will provide considerable advantages for a SDR application.

Acknowledgements:

The authors would like to thank J.R Macleod and P.A Warr for their useful comments and acknowledge Lucent Technologies for their financial support.

References:

[1] T. Nojima and T. Konno, Cuber predistortion lineariser for relay equipment in 800 MHz band land mobile telephone system, IEEE Transactions on Vehicular Technology, vol. 34, no. 4, Pages: 169-177, November 1985.

[2] K.A. Morris and P.B. Kenington, A Broadband Linear Power Amplifier for Software Radio Applications, IEEE 48th Vehicular Technology Conference, Pages: 2150-2154, Ottawa, May 1998.

[3] P.B. Kenington, R.J. Wilkinson and J. Marvill, "Broadband Linear Amplifier Design for a PCN Base-Station", Proc. of the 41st IEEE Conference on Veh. Technol., St. Louis, Missouri, May 1991, Pages: 155-160.

[4] T. Rahkonen, T. Kankaala, An analog predistortion integrated circuit for linearizing power amplifiers, Proceedings of Midwest Symposium on Circuits and Systems, 1999, Pages: 480–483.

[5] E. Westesson, L. Sundstrom, A complex polynomial predistorter chip in CMOS for baseband or IF linearization of RF power amplifiers, Proceedings of the 1999 IEEE International Symposium on Circuits and Systems, ISCAS '99, Volume: 1, Pages: 206–209.

[6] K.A. Morris and J.P. McGeehan, Gain and Phase Matching Requirements of Cubic Predistortion Systems, Electronics Letters, Vol. 36, No. 21, Pages: 1822-1824, October 2000.

[7] R. J. Wilkinson, P.B. Kenington, Specification of error amplifiers for use in feedforward transmitters, IEE Proceedings Circuits, Devices and Systems, Volume: 139 Issue: 4, Pages: 477–480, Aug. 1992.